Perpendicular interface resistances of sputtered Ag/Cu, Ag/Au, and Au/Cu multilayers

L. L. Henry,* Q. Yang, W.-C. Chiang, P. Holody, R. Loloee, and W. P. Pratt, Jr.
Department of Physics and Astronomy, and Center for Fundamental Materials Research, Michigan State University, East Lansing, Michigan 48824-1116

J. Bass†
Department of Physics and Astronomy, and Center for Fundamental Materials Research, Michigan State University, East Lansing, Michigan 48824-1116
and Grenoble High Magnetic Field Laboratory, Max-Planck-Institut für Festkörperforschung and CNRS, Boîte Postale 166, 38042 Grenoble Cedex 9, France

(Received 24 April 1996; revised manuscript received 29 July 1996)

We report measurements of the increase in perpendicular specific resistance (area times total resistance, AR_t) of multilayers of two nonmagnetic metals with increasing number of interfaces, when the total amount of each metal is held constant. For multilayers of Ag and Cu, Ag and Au, and Au and Cu sputtered under narrowly defined conditions, we find, per interface, $AR_{Ag/Cu}=0.044\pm0.003$ fΩ m^2; $AR_{Ag/Au}=0.050\pm0.004$ fΩ m^2; $AR_{Au/Cu}=0.149\pm0.006$ fΩ m^2. From independent estimates of the contributions to these values due to interface alloying, we conclude that such alloying can account for at least half and perhaps all of these values. These interface resistances are thus mostly not intrinsic. [S0163-1829(96)00542-5]

I. INTRODUCTION

Understanding the scattering of electrons at metallic interfaces is crucial to understanding giant (G) magnetoresistance (MR) in ferromagnetic metal–nonmagnetic metal (F/N) multilayers.[1] Historically, attention has focused on scattering for current flow parallel to surfaces or interfaces.[1,2] Recently, however, interest has begun to shift to the experimentally more challenging case of perpendicular incidence,[1,3] partly stimulated by new techniques[4,5] and measurements of the specific interface resistance, $AR_{F/N}$, the area A times perpendicular interface resistance, $R_{F/N}$, for Co/Ag,[4] Co/Cu,[6,7] and $Ni_{84}Fe_{16}$/Cu.[7]

Interface contributions to GMR have been attributed to spin-dependent scattering from:[1] (a) interface alloys; (b) interface roughness; (c) localized interface states; or (d) spin-dependent potential steps at the interface. The specific contribution from interface alloying should be easier to establish in N1/N2 multilayers, due to the absence of the spin dependence inherent in F/N multilayers. In this paper, we present the first measurements of $AR_{N1/N2}$ for N1/N2 multilayers—for Ag/Cu, Ag/Au, and Au/Cu, sputtered under various conditions. We examine how much of $AR_{N1/N2}$ can be ascribed simply to scattering from an interface alloy.

We chose Cu, Ag, and Au, for several reasons. (1) They have simple Fermi surfaces that are similar in form,[8] so that intercomparisons should not be complicated by very different electronic structures. (2) They sputter easily with little contamination. (3) They span a wide range of solubilities[9] and resistivity increases per atomic percent impurity, $\Delta\rho_0/\Delta c$.[10]

II. SAMPLE PREPARATION AND CHARACTERIZATION

Figure 1(a) shows a simplified schematic drawing of a sample and Fig. 1(b) shows the layering schematically. The N1/N2 multilayer is sandwiched between two 6 nm thick Co layers, outside of which are two crossed superconducting Nb strips, each 1.1 mm wide. The Co layers eliminate any proximity effect between the Nb and the multilayer.[11] The Nb strips are equipotentials, since Nb superconducts at our measuring temperature of 4.2 K. The ''short-wide'' sample geometry (length/width $\approx10^{-3}$) then ensures that essentially all of the current injected into one strip passes through the overlap area $A\approx1.25$ mm^2 and out of the other strip, giving a uniform current through A.[12] Using a reference resistor and superconducting quantum interference device-based measuring system, the total sample resistance R_t is measured with an uncertainty of about 1%. The measuring uncertainty in AR_t is ≈2–5 %, dominated by the uncertainty in the Nb strip widths.[4]

The samples are made in a computer-controlled, cryopumped, UHV compatible, sputtering system,[12] with a base pressure $\leqslant2\times10^{-8}$ Torr. All data shown are for samples sputtered at an argon pressure ≈2.5 mTorr, but a few Ag/Cu multilayers sputtered at 13 mTorr gave results similar to those shown. A 300 nm thick, bottom Nb strip is first sput-

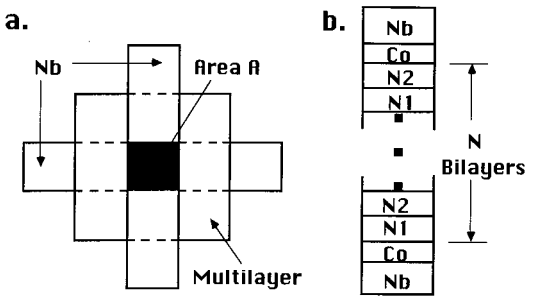

FIG. 1. (a) Sample schematic drawing. (b) Layering schematic drawing.

TABLE I. Various properties of the metal pairs.

Metals	Ag(1)/Cu(2)	Ag(1)/Au(2)	Au(1)/Cu(2)
1[a] ρ_{N1}; ρ_{N2} (nΩ m;nΩ m)	7±2; 6±2	7±2; 13±3	13±3; 6±2
2[b] Solubilities	Small	100%	Large
3[c] $\Delta\rho_0/\Delta c$ (nΩ m/at. %)	0.7?; 1.4?	3.6; 3.5	4.3; 5.3
4[d] ρ(50%) (Indep. Msmt.) (nΩ m)	19?	90	140
5[e] ρ(50%) (Nordh.) (nΩ m)	26?	89	120
6[f] ρ(50%) (Sputt. films) (nΩ m)	42±13	100±20	170±30
7[g] $\rho(50\%)\equiv\Delta(AR_t)/t_T$ (nΩ m)	51±9	86^{+13}_{-5}	125±12
8[h] ρ_{BE} (50%) (nΩ m)	42±10	90±10	140±20
9[i] t_{Ix} (nm)	0.5	0.5	0.4
10[j] t_{Ie} (nm)	0.9±0.2	0.6±0.1	1.2±0.2

[a]From measurements on 300 nm thick films.
[b]Reference 9.
[c]From Ref. 10. Listed first is N2 and N1, then N1 in N2. ?=large uncertainty.
[d]From Ref. 17: Ag/Au, uniform alloy; Au/Cu, rapidly quenched alloy (slow cooling gives an ordered alloy with much lower ρ); Ag/Cu, two-phase mixture.
[e]Estimated from the Nordheim equation [Eq. (4) in text] using the average of the $\Delta\rho_0/\Delta cs$ for the two metals (see row 3).
[f]From sputtered multilayer films with 0.5–1.0 ML thick layers (see text).
[g]From the data in Fig. 2 (see text).
[h]Best estimate from the information in rows 4–7 (see text).
[i]From x rays (see text).
[j]From Fig. 2 (see text).

tered through a strip mask. In 1–2 min, this mask is replaced, *in situ*, by a ''sample'' mask. A 6 nm thick Co layer is sputtered, then the multilayer, composed of N bilayers of metals N1 and N2, and finally a 6 nm thick Co capping layer. The sample mask is then exchanged for a strip mask perpendicular to the first one, and a 300 nm thick, top Nb strip is sputtered. Except for the very thinnest N1 and N2 layers, most of each layer is deposited while the substrate is at rest above a sputtering gun. However, some deposition occurs during the fraction of a second that the substrate moves into and out of the sputtering plume. The computer program takes this additional deposition into account in setting the time a substrate stays over each target. Most samples had total thickness t_T=360 nm, but several of each set were made with t_T=540 nm to check that a different total thickness gave compatible results.

The samples were sputtered onto c-axis oriented, single-crystal sapphire substrates, the temperatures of which were held above −50 °C and below 30 °C. The sputtering targets were ~5.5 cm in diameter and ~0.6 cm thick, made from 99.99% pure metals. The standard deposition rates were 1.0–1.25 nm/s for Ag, 1.2–1.35 nm/s for Cu, and 1.0–1.1 nm/s for Au. To reduce the importance for thinner layers of computer corrections for entrance and exit times, we also used ''half'' deposition rates, achieved by reducing the sputtering voltage.

Layer thicknesses were checked by both low- and high-angle ϑ–2ϑ x-ray scattering. We usually saw a single low-angle superlattice peak and both low-side and high-side high angle satellites about central peaks indicating (111) texture. The peak and satellite separations usually gave lengths agreeing with the intended bilayer thicknesses to within a few percent.

Attempts to derive interface alloying thicknesses t_I from computer fits of the high-angle satellite relative amplitudes were unsuccessful; the fits were insensitive to such alloying. We are thus limited to estimating bounds on t_I from the layer thicknesses at which we do and do not see low-angle superlattice peaks. We define t_{Ix} as the smallest layer thickness at which x rays still show such a peak. This definition yielded the values t_{Ix}=0.5 nm for Ag/Cu and Ag/Au, and 0.4 nm for Au/Cu, which we list in row 9 of Table I. These values of t_{Ix} correspond to only about 2 monolayers (ML) of each metal—the (111) interplanar spacings are 0.20 nm for Cu and 0.22 nm for Ag and Au—as small as they could possibly be, given that we cannot stop and start sputtering at the ends of individual layers. They are also smaller than the interface thicknesses suggested by other measurements of different multilayers sputtered in our system.[13] Analysis of a linear interface alloying profile (see below) shows that x-ray satellites should still be seen even for a layer thickness smaller than the t_I appropriate for calculating the interface resistance [see Eq. (3) below]. We, thus, view t_{Ix} as a lower bound on t_I.

III. THEORY

To isolate $AR_{N1/N2}$, we fix t_T, set the metal layer thicknesses $t_{N1}=t_{N2}=t_T/2N$, and vary only the bilayer number N. So long as quantum interference can be neglected, and the layer properties do not vary with their thicknesses, AR_t for the sample in Fig. 1(b) should be self-averaging, i.e., given simply by the series sum of the resistivities times layer thicknesses, ρt, for each layer, and of the AR's for each interface, independent of the sizes of the electron mean free paths in the layers:[4,14]

$$AR_t = 2AR_{\mathrm{Nb/Co}} + 2\rho_{\mathrm{Co}}(6\ \mathrm{nm}) + AR_{\mathrm{Co/N1}} + AR_{\mathrm{Co/N2}} + \rho_{\mathrm{N1}}(t_T/2) + \rho_{\mathrm{N2}}(t_T/2) + (2N-1)AR_{\mathrm{N1/N2}}. \quad (1)$$

Equation (1) should be valid if $AR_{\mathrm{N1/N2}}$ represents either an interface of negligible thickness, or one of finite thickness t_I' due to interface alloying. In the latter case, $AR_{\mathrm{N1/N2}}$ is the increase in AR_t due to alloying, above and beyond $\rho_{\mathrm{avg}} t_I'$, where ρ_{avg} is the average of the resistivities of N1 and N2. If Eq. (1) applies, a plot of AR_t vs N should give a straight line with ordinate intercept just the sum of the first six terms minus $AR_{\mathrm{N1/N2}}$, and slope $2AR_{\mathrm{N1/N2}}$. To check its applicability, independent measurements of each of the first six terms were made on similarly sputtered sandwiches and thin films, giving; $2AR_{\mathrm{Nb/Co}} = 6.1^{+1}_{-0.3}$ fΩ m^2;[15] $\rho_{\mathrm{Co}} = 50 \pm 10$ nΩ m; $\rho_{\mathrm{Ag}} = 7 \pm 2$ nΩ m; $\rho_{\mathrm{Cu}} = 6 \pm 2$ nΩ m; $\rho_{\mathrm{Au}} = 13 \pm 3$ nΩ m;[16] and $AR_{\mathrm{Co/N1}}$ and $AR_{\mathrm{Co/N2}}$—the interface resistances between Co and N1 and N2—$\approx 0.25 \pm 0.05$ fΩ m^2 each.[4,6] For $t_T = 360$ nm, including our derived values of $AR_{\mathrm{N1/N2}} \leqslant 0.15$ fΩ m^{-2} (see below), the ordinate intercepts of Eq. (1) are predicted to be $9.5^{+1.9}_{-1.2}$ fΩ m^2 for Ag/Cu, $10.8^{+2.1}_{-1.4}$ fΩ m^2 for Ag/Au, and $10.5^{+2.1}_{-1.4}$ fΩ m^2 for Au/Cu. For $t_T = 540$ nm, they should be just over 1 fΩ m^2 larger for Ag/Cu and slightly less than 2 fΩ m^2 larger for Au/Ag and Au/Cu.

When the interfaces begin to overlap, the rate of increase of AR_t with N should slow, and AR_t should saturate when the sample reaches a uniform 50–50 % alloy. In this state, the last term in Eq. (1) should be replaced by the constant term

$$\Delta(AR_t) = \rho(50\%) t_T, \quad (2)$$

where $\rho(50\%)$ is the resistivity of a 50–50 % alloy. We will use Eq. (2) to help establish $\rho(50\%)$, one of the two parameters we need to estimate $AR_{\mathrm{N1/N2}}$, as we now describe.

If interface alloying fully determines $AR_{\mathrm{N1/N2}}$, and if the alloy profile is a constant 50% of both metals over a thickness t_I (square profile), then the interface specific resistance is just

$$AR_{\mathrm{N1/N2}} = \rho(50\%) t_I. \quad (3)$$

In this case, to estimate $AR_{\mathrm{N1/N2}}$ due to alloying, we need values for $\rho(50\%)$ and t_I.

When the profile is not square, we can still write $AR_{\mathrm{N1/N2}}$ in the form of Eq. (3), but t_I must then represent an effective thickness smaller than the real one, t_I', over which the nonuniform alloy actually extends. We evaluate also a continuous linear interface profile, both because it is easy to calculate and because the unknown profile probably lies between linear and square—closer to square in the middle and to linear at its edges. Estimating the resistance of a linear interface using Nordheim's rule,[17]

$$\Delta\rho(c) = (\Delta\rho_0/\Delta c)_{\mathrm{avg}}(c/100\%)(100\% - c), \quad (4)$$

the t_I needed for Eq. (3) to give the same $AR_{\mathrm{N1/N2}}$ as for a linear profile is $t_I = 2/3 t_I'$.

For a square interface profile, saturation will be abrupt, and the common $t_{\mathrm{N1}} = t_{\mathrm{N2}}$ at which saturation occurs will be t_I. For a nonsquare profile, AR_t will saturate more gradually. For the linear profile, the value of t_I to be used in Eq. (3) is given by the $t_{\mathrm{N1}} = t_{\mathrm{N2}}$ at which the extrapolation of the linear slope of Eq. (1) intersects the saturation value of AR_t. This value occurs at $t_I \approx 2/3 t_I'$. As noted above, such a profile is still nonuniform for layers thinner than t_I, and thus still gives x-ray satellites.

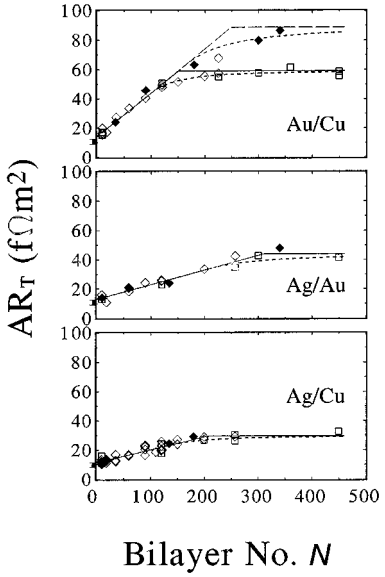

FIG. 2. The AR_t vs bilayer number N for Au/Cu, Ag/Au, and Ag/Cu multilayers sputtered at standard (diamonds) or half (squares) rates. Open symbols are for samples with $t_T = 360$ nm; filled ones are for $t_T = 540$ nm. The solid lines are ''square'' interface profile fits to the $t_T = 360$ nm data. The broken curve for Au/Cu is an extension of the parameters for the solid line to $t_T = 540$ nm. The dashed curves are for linear interface profiles with the same slopes and saturation values as for the solid lines. The black bars just left of the ordinate axes indicate the ranges of allowed intercepts given the uncertainties in the first six terms in Eq. (1).

In Sec. IV, we fit each data set with both a square profile and a linear profile having the same slope and same saturation value of AR_t as the square one.

IV. DATA

Figure 2 shows AR_t versus N for our three metal pairs using the two sputtering rates listed above. For each pair, the samples were sputtered in several separate runs. Where their data overlap, we found no obvious differences in AR_t for samples sputtered at ''standard'' (diamonds) or half rates (squares). The dark bands on the ordinate axes indicate the ranges of allowed sums of the constant terms in Eq. (1), for $t_T = 360$ nm, from the values given above.

The data of Fig. 2 are qualitatively consistent with Eq. (1) for each metal pair—they initially increase linearly with N and the data for $t_T = 360$ nm eventually level off as expected for overlapping interfaces. In the linear regions, we see no systematic differences between data for $t_T = 360$ nm (open symbols) or 540 nm (filled symbols). There, the data for 540 nm should be only 1–2 fΩ m^2 higher than for 360 nm, comparable to our measuring uncertainty. The linear regimes for 540 nm extend to larger N, because each N involves 50% thicker layers.

Since our interface alloying profiles are unlikely to be perfectly square, our data ought to approach saturation gradually instead of abruptly. In Fig. 2, the data for Au/Cu

TABLE II. Estimates and measurements of AR_{N1N2}.

Metals	Ag(1)/Cu(2)	Ag(1)/Au(2)	Au(1)/Cu(2)
1[a] $AR^{LB}_{N1N2}=\rho_{BE}$ (50%) t_{Ix} (fΩ m^2)	0.021±0.005	0.045±0.005	0.056±0.01
2[b] $AR^{est}_{N1N2}=\rho_{BE}$ (50%) t_{If} (fΩ m^2)	0.038±0.015	0.054±0.015	0.17 ±0.05
3[c] AR^{exp}_{N1N2} (fΩ m^2)	0.044±0.003	0.050±0.004	0.149±0.006

[a]Lower bound estimate: calculated from rows 8 and 9 in Table I.
[b]Estimate: calculated from rows 8 and 10 in Table I.
[c]Experimental: calculated from solid lines in Fig. 2.

require such a gradual approach, but those for Ag/Au and Ag/Cu can be either gradual or abrupt, depending upon the maximum value of N chosen for the linear regime. We examine both possibilities.

First, we force linear fits up to the largest values of N consistent with the scatter in the data, and determine the ''saturation values'' of AR_t by simply linearly averaging the values of AR_t for those data points that are consistent with saturation. As indicated in Sec. III, the values of N where the linear regimes intersect the saturation values of AR_t—which we designate by N_I—yield values of $t_{Ie}=t_T/2N_I$ that should approximate t_I. The solid lines in Fig. 2 are such fits for $t_T=360$ nm for Ag/Au (up to $N=257-N_I=311$), Ag/Cu (up to $N=200-N_I=208$), and Au/Cu (up to $N=120-N_I=151$). Their intercepts and slopes (with least-squares fit uncertainties) are $(11.4\pm0.5)+(0.088\pm0.005)N$ fΩ m^2 for Ag/Cu, $(13.1\pm1.0)+(0.100\pm0.008)N$ fΩ m^2 for Ag/Au and $(14.1\pm0.8)+(0.298\pm0.012)N$ fΩ m^2 for Au/Cu. Half the slopes give the values of $AR_{N1/N2}$ listed in row 3 of Table II. The best fit intercepts lie near or above the upper bounds estimated in Sec. III (11.4 fΩ m^2 for Ag/Cu, 12.9 fΩ m^2 for Ag/Au, and 12.6 fΩ m^2 for Au/Cu) from independent measurements of the first six terms in Eq. (1). However, including uncertainties gives overlap with the independent values, except for Au/Cu. An analysis of these slopes and intercepts using Eq. (1) is, thus, just internally consistent. We do not know if this bias toward high intercepts is due to slight variation of the ''constant'' terms of Eq. (1) with decreasing layer thickness, or if our choices of maximum N for the linear fits are too large. The values of t_{Ie} (listed in row 10 of Table I) found from the intercepts of the straight lines with the saturation values of AR_t are larger than the ''lower bound'' x-ray estimates of t_{Ix} given in row 9 of Table I, but are comparable to what we would have expected based upon the limitations of sputtering and measurements on other multilayers sputtered in our system.[13]

Second, we assume that all three sets of data approach saturation gradually, and fit the linear model noted in Sec. III (dashed curves in Fig. 2) to the same slopes and saturation values as for the square model. This model fits the Au/Cu data better than the square model does, and is consistent with the Ag/Cu and Ag/Au data sets to within their uncertainties.

Lastly, the parameters for $t_T=360$ nm let us predict square and linear profile behaviors for the $t_T=540$ nm Au/Cu data (broken and dashed curves, respectively), where those data extend farther in N than the $t_T=360$ nm data. The linear profile fits the $t_T=540$ nm data better.

V. ANALYSIS

We wish to examine how well interface alloying alone can account for the values of $AR_{N1/N2}$ listed in row 3 of Table II. More specifically, we ask what fractions of the values of $AR_{N1/N2}$ are given by Eq. (3). For this comparison, we need ''best values'' of $\rho(50\%)$ and t_I. We make four separate estimates of $\rho(50\%)$.

The first involves independent measurements of $\rho(50\%)$ for these alloys by others, as listed in row 4 of Table I.[18] The values for Ag/Au and Au/Cu should be reliable, as they represent true alloys. That for Ag/Cu is much less sure, as it represents a two phase mixture.

Alternatively, we can estimate $\rho(50\%)=25(\Delta\rho_0/\Delta c)_{avg}$ by combining Eq. (4) with the average of the $\Delta\rho_0/\Delta cs$ for N1 and N2 given in row 3 of Table I.[10] These estimates are listed in row 5 of Table I. Again, those for Ag/Au and Au/Cu should be reliable, as there are consistent independent measurements of $\Delta\rho_0/\Delta c$, while that for Ag/Cu is uncertain since the few independent measurements of $(\Delta\rho_0/\Delta c)$ scatter widely.[10]

Thirdly, we have approximated 50%/50% alloys experimentally ourselves by sputtering, onto silicon substrates, multilayer films with intended layer thicknesses of only 0.5–1.0 ML, thin enough to minimize any effects of layering. This process required reducing our sputtering rates to about 1/5 standard, which led to higher average resistivities for single metal films sputtered at similarly slow rates. Our best estimates of $\rho(50\%)$ for these films, after subtracting $\rho_{avg}t_I$ for the two metallic constituents to correct for additional defects in the sputtered alloy films,[16] are given in row 6 of Table I. Here, the estimates for Ag/Cu and Ag/Au should be reliable, as they involve averages over several films each, whereas that for Au/Cu is less sure, as it is based on only a single film.

Lastly, we estimate $\rho(50\%)$, by combining the data of Fig. 2 with Eq. (2). These estimates, which are independent of the interface profile, are given in row 7 of Table I.

Comparing the four estimates of $\rho(50\%)$ in rows 4–7, we find that they all agree well for Ag/Au, are roughly consistent for Au/Cu, and divide into two groups for Ag/Cu. From these observations, we infer that $\rho(50\%)=90\pm10$ nΩ m for Ag/Au and 140 ± 20 nΩ m for Au/Cu should be reliable approximations. For Ag/Cu, the values from our measurements on sputtered films with very thin layers (row 6) and on our multilayers (row 7) are about twice those estimated from the independent measurements on alloys (row 4) and from Nordheim's rule (row 5). However, the $\rho(50\%)$ in row 5 is for a two-phase mixture,[18] and the estimates for $(\Delta\rho_0/\Delta c)$ used in

Eq. (4) are not well reproduced.[10] We thus weight the other two values most heavily and choose $\rho(50\%)=42\pm10$ nΩ m. Our three ''best estimates'' are given in row 8.

Turning now to t_I, in Sec. II we estimated from x-ray studies the lower bound values of t_{Ix} listed in row 9 of Table I, and in Sec. IV we estimated from the data of Fig. 2 the value of t_{Ie} given in row 10 of Table I. Combining the lower bound estimates of t_{Ix} with our best estimates of $\rho(50\%)$ in row 8 of Table I gives the lower bound estimates of $AR_{\mathrm{N1/N2}}$ listed in row 1 of Table II. These estimates account for 40–90 % of our best values for $AR_{\mathrm{N1/N2}}$. We conclude that at least 40–90 % of the respective values of $AR_{\mathrm{N1/N2}}$ are due simply to interface alloying. If, instead, we combine the values of t_{Ie} in row 10 of Table I with our best estimates for $\rho(50\%)$ in row 8, we obtain the $AR_{\mathrm{N1/N2}}$ predictions listed in row 2 of Table II. These predictions overlap our best values of $AR_{\mathrm{N1/N2}}$ in row 3.

VI. SUMMARY AND CONCLUSIONS

In summary, our measurements of the increase in perpendicular specific resistance, AR_t, of sputtered N1/N2 multilayers yield interface specific resistances of $AR_{\mathrm{Ag/Cu}}=0.044\pm0.003$ fΩ m^2, $AR_{\mathrm{Ag/Au}}=0.050\pm0.004$ fΩ m^2, and $AR_{\mathrm{Au/Cu}}=0.149\pm0.006$ fΩ m^2. From independent estimates of $\rho(50\%)t_I$, we find that interface alloying accounts for 40–100 % of $AR_{\mathrm{Au/Cu}}$, 50–100% of $AR_{\mathrm{Ag/Cu}}$, and 90–100% of $AR_{\mathrm{Ag/Au}}$. For multilayers in which such a large fraction of $AR_{\mathrm{N1/N2}}$ is due to interface alloying, there is no unique interface specific resistance, in that different preparation conditions can give different interface thicknesses.

We end by comparing our values of $AR_{\mathrm{N1/N2}}$ for Ag/Cu, Ag/Au, and Au/Cu with those for the S/F pair Nb/Co ($AR_{\mathrm{Nb/Co}}\cong3$ fΩ m^2) and for three F/N metal pairs, Co/Cu, Co/Ag, and Py/Cu.[19] $AR_{\mathrm{N1/N2}}$ is much smaller than $AR_{\mathrm{Nb/Co}}$, where the physics determining AR is presumably quite different.[15] The comparisons with the F/N pairs can only be rough, since an F/N interface does not have a unique specific resistance; rather, there are separate AR's for majority and minority carriers, and different combinations for different magnetic structures of the multilayer. As the noble metals have high conductivities, we choose $AR\uparrow_{\mathrm{F/N}}$ for the highest conductivity electrons.[4,14,19] This is the lowest possible value for the comparison. We also reduce the values of $AR\uparrow_{\mathrm{F/N}}$ by half, assuming that they are due to only half the conduction electrons. The resulting values of $(AR\uparrow_{\mathrm{Co/Cu}}/2)\cong0.13$ fΩ m^2, $(AR\uparrow_{\mathrm{Co/Ag}}/2)\cong0.1$ fΩ m^2, and $(AR\uparrow_{\mathrm{Py/Cu}}/2)\cong0.09$ fΩ m^2, are comparable to those for $AR_{\mathrm{N1/N2}}$ for our noble-metal pairs. Further investigations must determine if the physics underlying them is also the same.

ACKNOWLEDGMENTS

This research was supported in part by the NSF through Grants No. DMR-91-22614 and DMR-94-623795, by the MSU-CFMR, and by the MPI Stuttgart and the MPI/CNRS High Magnetic Field Laboratory in Grenoble, France, where part of this paper was drafted. The authors also thank P. A. Schroeder, P. M. Levy, A. Fert, H. Sato, V. S. Tsoi, and S. D. Mahanti for helpful suggestions, and D. Baxter for use of his x-ray facility at Indiana University.

*Present address: Physics Department, Southern University and A&M College, Baton Rouge, LA.

†To whom correspondence should be sent at MSU.

[1] R. Q. Hood and L. M. Falicov, in *Magnetic Ultrathin Films, Multilayers and Surfaces/Interfaces and Characterization*, edited by B. T. Jonker, S. A. Chambers, R. F. C. Farrow, C. Chappert, R. Clarke, W. J. M. de Jonge, T. Egami, P. Grünberg, K. M. Krishnan, E. E. Marinero, C. Rau, and S. Tsunashima, MRS Symposia Proceedings No. 313 (Materials Research Society, Pittsburgh, 1993), p. 23; P. M. Levy *et al.*, Magnetic Structures in Systems of Reduced Dimension, edited by R. C. Farrow *et al.* (Plenum, New York, 1993), p. 155; P. M. Levy, in *Solid State Physics*, edited by H. Ehrenreich and D. Turnbull (Academic, New York, 1994), Vol. 47, p. 367.

[2] Z. Tesanovic, M. V. Jaric, and S. Maekawa, Phys. Rev. Lett. **57**, 2760 (1986), and references therein.

[3] N. Trivedi and N. W. Ashcroft, Phys. Rev. B **35**, 6084 (1987); A. Brataas and G. E. W. Bauer, Europhys. Lett. **26**, 117 (1994): Y. Asano, A. Oguri, and S. Maekawa, Phys. Rev. B **48**, 6192 (1993); S. Zhang and P. M. Levy, in *Magnetic Ultrathin Films, Multilayers and Surfaces/Interfaces and Characterization*, edited by B. T. Jonker, S. A. Chambers, R. F. C. Farrow, C. Chappert, R. Clarke, W. J. M. de Jonge, T. Egami, P. Grünberg, K. M. Krishnan, E. E. Marinero, C. Rau, and S. Tsunashima, MRS Symposia Proceedings No. 313 (Materials Research Society, Pittsburgh, 1993), p. 53; J. Barnas and A. Fert, Phys. Rev. B **49**, 12 835 (1994).

[4] S.-F. Lee *et al.*, J. Magn. Magn. Mater. **118**, L1 (1993).

[5] M. A. M. Gijs *et al.*, Phys. Rev. Lett. **70**, 3343 (1993).

[6] W. P. Pratt, Jr. *et al.*, J. Magn. Magn. Mater. **126**, 406 (1993).

[7] P. A. Schroeder *et al.*, in *Magnetic Ultrathin Films, Multilayers and Surfaces/Interfaces and Characterization*, edited by B. T. Jonker, S. A. Chambers, R. F. C. Farrow, C. Chappert, R. Clarke, W. J. M. de Jonge, T. Egami, P. Grünberg, K. M. Krishnan, E. E. Marinero, C. Rau, and S. Tsunashima, MRS Symposia Proceedings No. 313 (Materials Research Society, Pittsburgh, 1993), p. 47; P. Holody (unpublished).

[8] A. P. Cracknell, Adv. Phys. **20**, 1 (1971).

[9] M. Hanson and K. Anderko, *Constitution of Binary Alloys*, 2nd ed., Metallurgy and Metallurgical Engineering Series, edited by R. P. Mehl (McGraw-Hill, New York, 1958), R. Elliott, *ibid.*, 1st Suppl., 1965.

[10] J. Bass, in *Metals: Electronic Transport Phenomena*, edited by K.-H. Hellwege and J. L. Olsen, Landolt-Bornstein New Series, III/15a (Springer-Verlag, Berlin, 1982).

[11] J. M. Slaughter *et al.*, Jpn. J. Appl. Phys. **26**, Suppl. 26-3, 1451 (1987).

[12] J. M. Slaughter *et al.*, Rev. Sci. Instrum. **60**, 127 (1989).

[13] R. Stubi *et al.*, Europhys. Lett. **19**, 235 (1992); P. Panissod and C. Meny, J. Magn. Magn. Mater. **126**, 16 (1993); E. A. M. van Alphen *et al.*, J. Appl. Phys. **76**, 6607 (1994).

[14] S. Zhang and P. M. Levy, J. Appl. Phys. **69**, 4786 (1991); T. Valet and A. Fert, Phys. Rev. B **48**, 7099 (1993); H. E. Camblong, S. Zhang, and P. M. Levy, J. Appl. Phys. **75**, 6909 (1994).

[15] C. Fierz *et al.*, J. Phys. Condens. Matter **2**, 9701 (1990).
[16] L. L. Henry *et al.* (unpublished).
[17] P. L. Rossiter and J. Bass, in *Materials Science and Technology*, edited by K. H. J. Buschow (VCH, Weinheim, 1992), Vol. 3A, p. 257.
[18] K. Schroder, *CRC Handbook of Electrical Resistivities of Binary Metallic Alloys* (CRC, Boca Raton, FL, 1983).
[19] J. Bass *et al.*, Mater. Sci. Eng. B **31**, 77 (1995), and references therein.